THE JOURNAL OF BIOLOGICAL CHEMISTRY VOL. 286, NO. 27, pp. 23780–23788, July 8, 2011

Substrate-dependent Gating of Anion Channels Associated with Excitatory Amino Acid Transporter 4*

Received for publication, November 30, 2010, and in revised form, May 6, 2011 Published, JBC Papers in Press, May 13, 2011, DOI 10.1074/jbc.M110.207514

Jan-Philipp Machtens, Peter Kovermann, and Christoph Fahlke[1]

From the Institut für Neurophysiologie, Medizinische Hochschule, 30625 Hannover, Germany and the Zentrum für Systemische Neurowissenschaften Hannover (ZSN), 30559 Hannover, Germany

EAAT glutamate transporters do not only function as secondary-active glutamate transporters but also as anion channels. EAAT anion channel activity depends on transport substrates. For most isoforms, it is negligible without external Na^+ and increased by external glutamate. We here investigated gating of EAAT4 anion channels with various cations and amino acid substrates using patch clamp experiments on a mammalian cell line. We demonstrate that Li^+ can substitute for Na^+ in supporting substrate-activated anion currents, albeit with changed voltage dependence. Anion currents were recorded in glutamate, aspartate, and cysteine, and distinct time and voltage dependences were observed. For each substrate, gating was different in external Na^+ or Li^+. All features of voltage-dependent and substrate-specific anion channel gating can be described by a simplified nine-state model of the transport cycle in which only amino acid substrate-bound states assume high anion channel open probabilities. The kinetic scheme suggests that the substrate dependence of channel gating is exclusively caused by differences in substrate association and translocation. Moreover, the voltage dependence of anion channel gating arises predominantly from electrogenic cation binding and membrane translocation of the transporter. We conclude that all voltage- and substrate-dependent conformational changes of the EAAT4 anion channel are linked to transitions within the transport cycle.

Excitatory amino acid transporters (EAATs)[2] comprise a family of glial and neuronal glutamate transporters that are crucial for termination of glutamatergic synaptic transmission and for maintenance of low resting glutamate levels (1–3). EAAT-mediated glutamate transport is stoichiometrically coupled to the movement of three sodium ions and one proton, while one potassium ion is counter-transported (4, 5). EAATs remove glutamate from the synaptic cleft and its surrounding as stoichiometrically coupled co-transporters of one glutamate, three sodium ions, and one proton, whereas one potassium ion is counter-transported (4, 5). However, EAATs are not only secondary-active glutamate transporters but also anion-selective channels (6). For some EAAT isoforms, anion currents are much smaller than the electrogenic uptake currents. For others, anion currents represent the predominant transporter-mediated current component (7–10). These differences suggest that some EAATs might play a physiological role as substrate-gated anion channels involved in the regulation of cellular excitability and others as glutamate transporters (11, 12).

EAAT anion channels have been functionally characterized in detail (7, 8, 10, 12–16). Many experimental results support a model in which only certain carrier conformations are associated with conducting anion pores, and the anion channel cycles between conducting and non-conducting states during transitions through various conformational states of the glutamate transporter (14, 17). This tight coupling predicts that the voltage dependence of EAAT anion currents exclusively arises from transitions between different carrier conformations and that kinetic properties of EAAT transporters might be extracted from EAAT anion currents. Indeed, all current kinetic models are based on such measurements (14, 18, 19). However, defining kinetic parameters from anion currents is only possible if all channel states are directly associated with the uptake cycle. This has been questioned by recent reports: for EAAT1 and EAAT3, Li^+ was reported to support coupled transport, but not anion channel function, indicating an additional Na^+-dependent conformational gating transition of EAAT anion channels beyond the uptake cycle (20, 21).

To further probe the existence of such conformational changes, we studied the substrate dependence of EAAT4 anion channels by comparing channel gating in Na^+ and Li^+ as well as in glutamate, aspartate, and cysteine. We observed distinct anion channel gating for the three amino acid substrates. Our data can be described by a kinetic scheme in which the substrate dependence of EAAT4 anion channels is entirely due to differences in substrate and cation association and translocation.

EXPERIMENTAL PROCEDURES

Expression in Mammalian Cells—Rat EAAT4 and human EAAT1 were expressed in mammalian cells as fusion proteins containing an amino-terminal fluorescent protein. Expression constructs were generated by directly linking the coding regions of monomeric yellow fluorescent protein to rat EAAT4 (kindly provided by Dr. J. Rothstein, Johns Hopkins University, Baltimore, MD) via a BsrGI restriction site into an open reading frame and subcloned into pcDNA3.1(−) using flanking BamHI and BsgI restriction sites. The BsrGI site was created by introduction of a silent mutation with PCR. A comparable construct encoding human EAAT1 was formed by linking human EAAT1 (kindly provided by S. Amara, University of Pittsburgh, Pitts-

* This work was supported by the Deutsche Forschungsgemeinschaft (FA301/9 to Ch. F.).

[1] To whom correspondence should be addressed: Christoph Fahlke, Institut für Neurophysiologie, Medizinische Hochschule, Hannover, Carl-Neuberg-Strasse 1, D-30625 Hannover, Germany. Tel.: 49-511-532-2777; Fax: 49-511-532-2776; E-mail: fahlke.christoph@mh-hannover.de.

[2] The abbreviation used is: EAAT, excitatory amino acid transporter.

burgh, PA) via an AgeI site with YFP into an open reading frame and subcloning into pcDNA3.1(+) using EcoRI and XbaI.

Transient transfection of HEK293T cells using the $Ca_3(PO_4)_2$ technique was performed as described previously (10). Measurements with two independent recombinants and a non-fluorescent construct (22) were compared and shown to exhibit indistinguishable functional properties.

Electrophysiology—Standard whole-cell patch clamp recordings were performed using an Axopatch 200B amplifier (Molecular Devices, Palo Alto, CA). Borosilicate pipettes were pulled with resistances between 1.0 and 1.5 megohms. Cells were clamped to 0 mV for at least 2 s between test sweeps. Voltage errors were reduced by compensating 80–90% of series resistance by an analog procedure and excluding cells with current amplitudes higher than 12 nA. Currents were low pass-filtered at 10 kHz and digitized at 50 kHz using a Bessel low pass filter and a Digidata 1322A AD/DA converter (Molecular Devices, Sunnyvale, CA).

Bath solutions contained 140 mM (Na/Li)NO_3, 20 mM L-glutamic acid/L-aspartic acid/L-cysteine, 4 mM KCl, 2 mM $CaCl_2$, 1 mM $MgCl_2$, 5 mM HEPES, 5 mM tetraethylammonium chloride. For titration experiments with varying amino acid concentrations, amino acids were substituted equimolarly with gluconic acid. Pipettes were filled with 115 mM (Na/K)NO_3, 20 mM gluconic acid, 2 mM $MgCl_2$, 5 mM EGTA, 10 mM HEPES. Sodium and lithium dependences were determined by equimolar substitution of external (Na/Li)NO_3 with choline NO_3 in the presence of 20 mM L-glutamate. In all solutions, pH was adjusted to 7.4 with *N*-methyl-glucamine. External and internal salt agar bridges were made from a plastic tube filled with 3 M KCl in 1.5% agar and used for electrical connection with the Ag/AgCl electrode.

Data Analysis—Data were analyzed with a combination of pClamp10 (Axon Instruments), MATLAB (version 7, MathWorks), and SigmaPlot (version 11, Jandel Scientific) programs. Current amplitudes were used without any subtraction procedure. Data are given as means ± S.E.

Current-voltage relationships were constructed by plotting steady-state current amplitudes *versus* the membrane potential. To analyze the concentration dependence of anion currents, steady-state currents at a given test potential were measured at various substrate or cation concentrations and fitted with the Hill equation. Concentration-response data were averaged after normalization to the maximum current extrapolated from fitted Hill functions. Instantaneous current amplitudes were determined by extrapolation of mono- or biexponential fits to the initial voltage step. Relative open probabilities were calculated from instantaneous tail currents at +135 mV plotted *versus* the prepulse potential after normalization to the maximum tail current observed in Na^+ and aspartate (22).

Kinetic Modeling—Simulations of EAAT4 anion currents were performed with self-written programs in the MATLAB environment. Differential equations according to the model (see Fig. 5*A*) were numerically solved using the stiff ode15s solver as implemented in MATLAB. Parameters were estimated by fitting the model simultaneously to experimentally determined relative open probabilities, time courses of current relaxations, concentration-response curves with Na^+ or Li^+ as well as with glutamate, aspartate, or cysteine. Residuals were minimized with the MATLAB Genetic Algorithm Toolbox. To account for differences observed with separate substrates, distinct rates for reactions 2, 3, 4 (forward/backward), and 5 (forward) were allowed for each amino acid (see Fig. 5*A*). As the combination of interacting substrates and cation determine the properties of the transporters (23), the model assumed different rate constants with each amino acid for reaction 3 with Na^+ or Li^+. To compare measured relative open probabilities with simulated absolute values, we found that an open probability of ~0.6 was the highest value the model could assume to correctly reproduce time-dependent channel gating (see Fig. 6). For the model optimization, we therefore normalized relative P_o to this value. Because we could not reliably estimate every reaction rate from our measurements, Na^+-dependent retranslocation rates (reaction 8) were taken from a kinetic model (14) that was recently successfully used to describe EAAT4 (22). Channel gating reactions were simplified as rapid pre-equilibria and defined by specific open probabilities that account for the equilibrium distribution between each state of the transport cycle and its associated channel mode Ch. Overall channel open probabilities (P_o) were calculated as sums of fractional occupancies in channel model Ch. Whole-cell anion currents (I) were then given with the published single-channel current (i) characteristics of EAAT4 (22), an arbitrarily chosen number of transporters (n = 77,000) and the relation $I(V) = N \cdot P(V) \cdot i(V)$. Relevant concentrations in all simulations were set to mimic experimental conditions. Apparent cation affinities in the presence of glutamate were calculated by fitting Hill functions to simulated concentration-response curves at various voltages (see Fig. 6, *D* and *E*).

RESULTS

Li^+ Supports Glutamate-activated EAAT4 Anion Currents—WT EAAT4 was heterologously expressed in HEK293T cells, and ionic currents were measured through whole-cell patch clamping (Fig. 1). Cells were dialyzed with Na^+-based solutions to suppress coupled transport and to reduce the number of relevant states of the transport cycle involved in anion channel gating. Substitution of Cl^- with NO_3^- increased anion currents up to 10-fold (10) and resulted in EAAT4 anion currents that largely exceeded endogenous currents (10, 22). These recording conditions thus permitted measurements of EAAT4 anion currents in isolation.

Fig. 1 shows representative current recordings in Na^+- or Li^+-based external solutions, either prior or after application of 20 mM L-glutamate. In the absence of glutamate, anion currents exhibit comparable amplitudes with Na^+ or with Li^+. Application of glutamate increases current amplitudes at negative as well as at positive voltages. In the presence of external Na^+ and glutamate, currents rise instantaneously upon voltage steps from 0 mV to negative as well as positive potentials and decay to steady-state levels within 30–60 ms (Fig. 1*A*) (22). With external Li^+, glutamate-induced currents are smaller and current relaxations following depolarization are slowed down. Exchange of Na^+ by Li^+ decreases steady-state current amplitudes to values between 40% (+180 mV) and 80% (−170 mV) of those observed in Na^+ and L-glutamate (Fig. 1*B*).

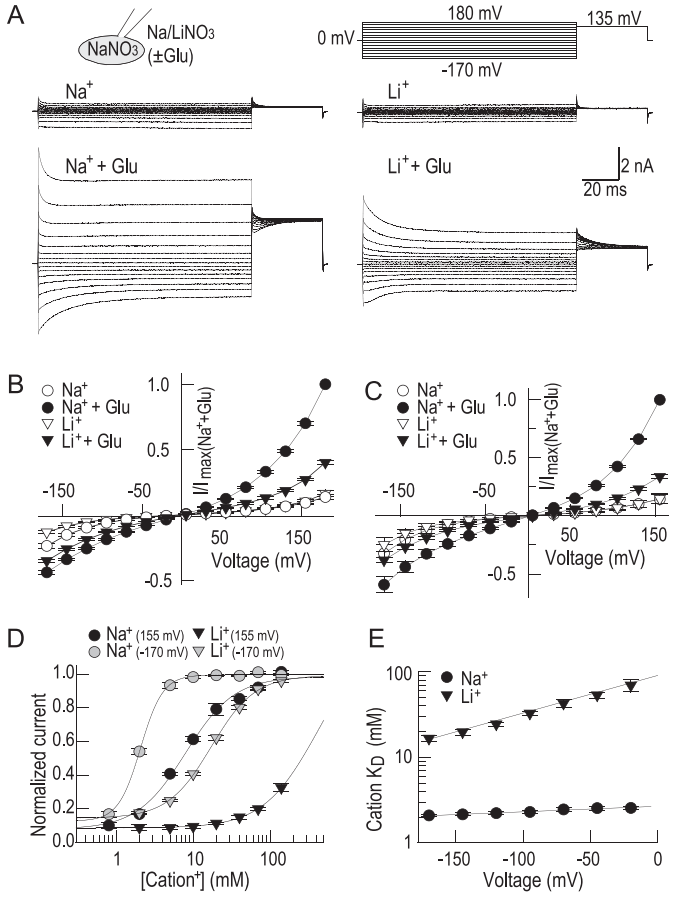

FIGURE 1. **Li^+ substitutes for sodium in activating EAAT4 anion currents.** *A*, representative current recordings from cells expressing EAAT4 in sodium and lithium-based bath solutions in the absence or presence of saturating concentrations of L-glutamate. *B* and *C*, current-voltage relationship of steady-state current amplitudes ($n = 4$) under standard $NaNO_3$-based (*B*) or KNO_3-based (*C*) internal solutions. *D*, concentration-response curves of steady-state currents with external sodium or lithium in the presence of 20 mM L-glutamate. After normalization, data were fitted with Hill equations with the following apparent K_D values for sodium: 2.1 ± 0.1 mM (−170 mV) and 8.6 ± 0.5 mM (+155 mV) with Hill coefficients ranging from 2.7 ± 0.2 (−170 mV) to 1.3 ± 0.1 (+155 mV); and for lithium, the apparent K_D values were as follows: 16.6 ± 1.2 (−170 mV) and >100 mM (+155 mV) and Hill coefficients of 1.5 ± 0.1 (−170 mV) ($n = 4$–7). *E*, voltage dependence of apparent cation affinities shown on the semi-log scale. Log(K_D) fitted with linear functions with slopes of 0.65 ± 0.05·10^{-3}/mV for sodium and 4.40 ± 0.32·10^{-3}/mV for lithium binding ($n = 4$–7).

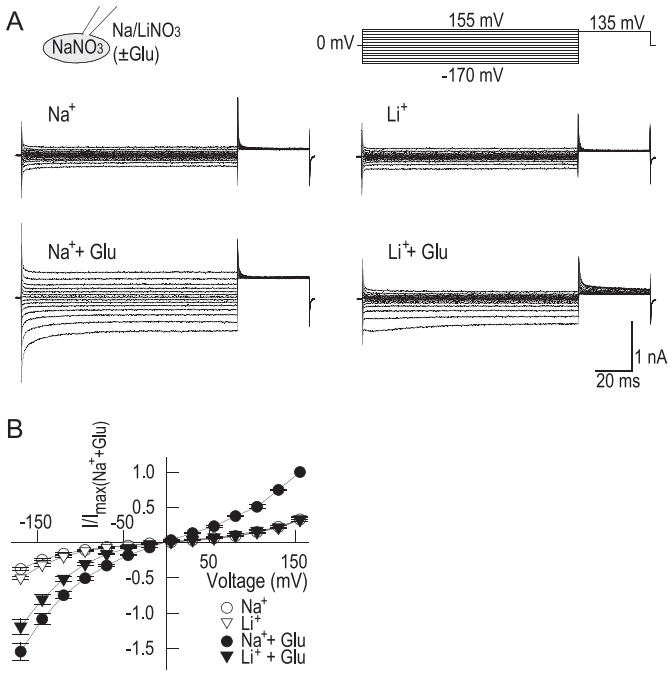

FIGURE 2. **Li^+ also sustains glutamate-activated anion currents in EAAT1.** *A*, representative current recordings from cells expressing EAAT1 in sodium- and lithium-based bath solutions in the absence or presence of saturating concentrations of L-glutamate (20 mM). Cells were dialyzed with $NaNO_3$-based pipette solutions. *B*, current-voltage relationship of steady-state current amplitudes ($n = 5$).

Our data differ from recent reports that Li^+ cannot support activation of EAAT1 and EAAT3 anion currents by glutamate (20, 21). A possible explanation for this discrepancy might be that Li^+ only activates EAAT anion channels in the presence of internal Na^+, however this is not the case. With KNO_3-based pipette solutions, EAAT4 current amplitudes were generally smaller, but glutamate-induced current increases were still detectable in the presence of external Na^+ as well as in Li^+ (Fig. 1*C*).

Fig. 1*D* gives concentration dependences of steady-state currents for Na^+ and Li^+ in the presence of glutamate. Because binding of cations and amino acid substrates depend on each other, glutamate was applied at a concentration of 20 mM to approximate saturation under all conditions. For Na^+ as well as for Li^+, concentration dependences could be well described with Hill functions. Titration with different [Na^+] revealed apparent K_D values of 2.1 ± 0.1 mM (at −170 mV) and 8.6 ± 0.5 mM (at +155 mV) with Hill coefficients ranging from 2.7 ± 0.2 (−170 mV) to 1.3 ± 0.1 (+155 mV) consistent with previous results (18, 22). Li^+ affinities were 8- to 40-fold reduced with apparent K_D values between 16.6 ± 1.2 (−170 mV, Hill coefficient 1.5 ± 0.1) and values > 100 mM (+155 mV).

Binding of Na^+ and Li^+ to the transporter is promoted by negative potentials. The association of Li^+ is apparently more voltage-dependent than that of Na^+ (Fig. 1*E*). The voltage dependence of both K_D values could be well described with a linear fit on a semi-logarithmic scale with a slope of 4.4 ± 0.3·10^{-3}/mV for Li^+ and 0.7 ± 0.1·10^{-3}/mV for Na^+ (Fig. 1*E*). As the determination of apparent K_D was less accurate at positive potentials due to the restricted concentration range in our experiments with Li^+, this analysis is only shown at negative potentials.

To test whether activation of EAAT4 anion channels in Li^+ is a unique feature of this particular isoform, we next studied EAAT1 anion currents in our experimental system (Fig. 2). In symmetrical NO_3^-, cells expressing EAAT1 exhibited glutamate-sensitive anion currents that differ from EAAT4 currents in their time and voltage dependence. In external glutamate, EAAT1 anion currents are inwardly rectifying (Fig. 2), in clear contrast to the outward rectification of EAAT4 currents (Fig. 1). With Li^+, glutamate still activates EAAT1 anion channels (Fig. 2, *A* and *B*). However, the ability of Li^+ to substitute for Na^+ differs markedly from EAAT4 in its voltage dependence. At negative potentials, glutamate-induced currents in Li^+ measure ~80% of those observed in Na^+ ($n = 5$). In contrast, glutamate was unable to increase current amplitudes in Li^+ at positive potentials (Fig. 2, *A* and *B*).

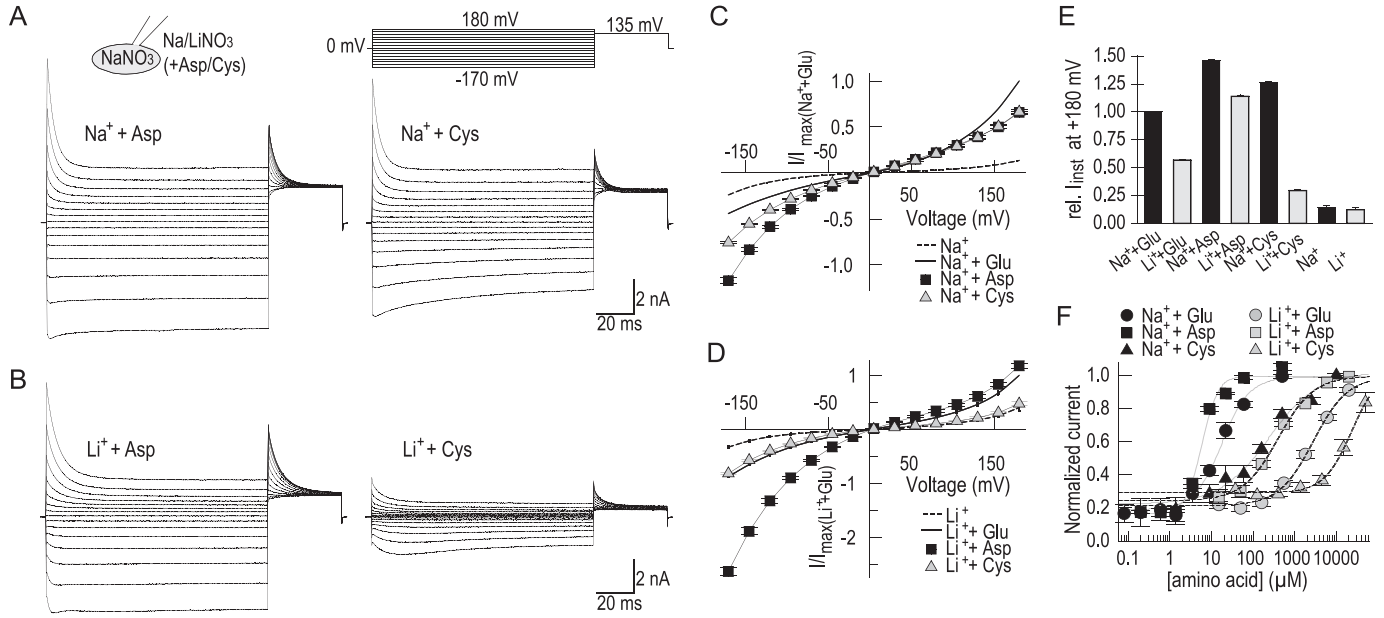

FIGURE 3. **Aspartate- and cysteine-elicited anion currents exhibit a changed phenotype of gating.** *A* and *B*, representative EAAT4 current recordings in Na^+-based (*A*) or Li^+-based (*B*) bath solutions with saturating concentrations of L-aspartate or L-cysteine. *C* and *D*, current-voltage relationship of steady-state current amplitudes in external Na^+- (*C*) or Li^+- (*D*) based solutions. Data are normalized to the respective maximum current in glutamate (+155 mV) ($n = 4$). Line plots represent data taken from Fig. 1. *E*, instantaneous current amplitudes after steps to +180 mV, normalized to current amplitudes measured at the same cell in external Na^+ and L-glutamate ($n = 4$). *F*, concentration-response curves of steady-state currents with L-glutamate, L-aspartate, and L-cysteine with external Na^+ or Li^+ at +155 mV ($n = 3–4$).

Aspartate- and Cysteine-elicited Anion Currents Display Changed Voltage Dependence of Gating—We next compared EAAT4 anion currents in the presence of other amino acid substrates, L-aspartate or L-cysteine, in combination with external Na^+ or Li^+. Applying voltage steps to cells perfused with Na^+ and saturating (20 mM) L-aspartate concentrations elicited large instantaneous current amplitudes at both negative and positive potentials (Fig. 3*A*). In contrast to glutamate, outward currents inactivated mainly, whereas inward currents remained relatively unchanged over time. Similar time and voltage dependences were observed upon perfusion with Na^+ and L-cysteine (20 mM). However, under these conditions, deactivation upon hyperpolarization was intermediate to results obtained under aspartate and glutamate conditions.

Aspartate-induced anion currents were only slightly modified by Li^+, whereas cysteine-elicited current amplitudes in Li^+ were up to 4-fold smaller compared with Na^+-containing media (Fig. 3*B*). In Na^+-based external solutions, steady-state currents are largest in the presence of glutamate at positive potentials and in aspartate at negative potentials (Fig. 3*C*). With external Li^+, the sequence of decreasing efficiency in initiating anion currents was aspartate > glutamate > cysteine at all potentials (Fig. 3*D*).

Comparison of instantaneous current amplitudes at +180 mV demonstrated that aspartate and cysteine are more effective substrates than glutamate in combination with Na^+ (Fig. 3*E*). In Li^+, instantaneous current amplitudes were large with aspartate but cysteine was found to be a very poor agonist. Nevertheless, currents were always larger in the presence of substrate than in its absence. Fig. 3*F* shows dose-response curves of steady-state currents for glutamate, aspartate, and cysteine in the presence of Na^+ or Li^+. At +155 mV in Na^+, these curves could be well fit with Hill functions with apparent K_D values of 16.6 ± 0.8 μM (L-glutamate), 5.7 ± 0.3 μM (L-aspartate), and 256 ± 21 μM (L-cysteine) and Hill coefficients of 1.2 ± 0.1 (L-glutamate), 2.1 ± 0.1 (L-aspartate), and 0.9 ± 0.1 (L-cysteine). In Li^+, these curves were shifted to K_D values of 2802 ± 246 μM (L-glutamate), 400 ± 25.3 μM (L-aspartate), and > 20 mM (L-cysteine) and Hill coefficients of 1.1 ± 0.1 (L-glutamate) and 1.0 ± 0.1 (L-aspartate).

Substrate-Cation Interactions Contribute to Voltage-dependent Channel Open Probabilities—To quantify the effect of different amino acid substrates on voltage-dependent gating, we calculated relative open probabilities by normalizing instantaneous tail currents at +135 mV to maximum current amplitudes with Na^+/aspartate and plotted the resulting values *versus* the preceding voltage for various substrate conditions (Fig. 4*A*, *inset*). We recently demonstrated that this approach provides similar results as direct measurements of anion channel open probabilities via noise analysis (22). With Na^+, relative open probabilities of EAAT4 with aspartate were ~0.3 at +180 mV but increased to 1.0 in the negative voltage range (Fig. 4*A*). Whereas EAAT4 acted similarly with cysteine and aspartate at positive voltages, open probabilities were significantly lower in cysteine below −50 mV. In glutamate, open probabilities were larger than in aspartate at positive potentials, but smaller at negative potentials, resulting in bell-shaped activation curves with a maximum ~0 mV (22). In the absence of any amino acid substrate, open probabilities decreased with almost linear voltage dependence from 0.2 at very negative to 0.1 at very positive potentials. Exchanging Na^+ with Li^+ left open probabilities with aspartate relatively unchanged (Fig. 4*B*). However, biphasic activation curves in the presence of glutamate were shifted to the left and reduced by ~30%. In the presence of Li^+, cysteine

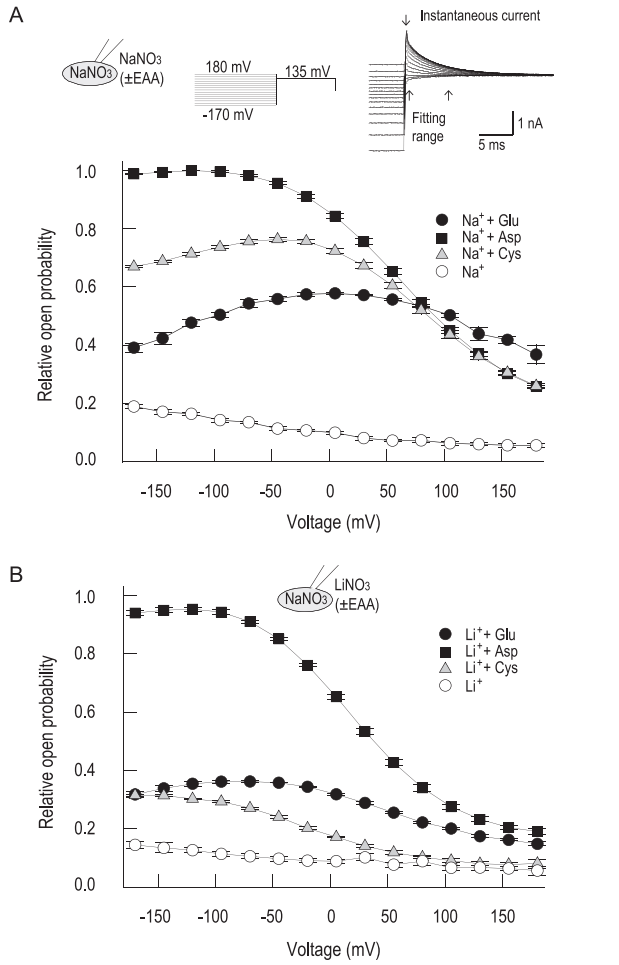

FIGURE 4. **Voltage dependence of relative open probabilities.** *A* and *B*, instantaneous tail current amplitudes upon voltage steps to +135 mV plotted against the preceding potential in Na^+- (*A*) or Li^+- (*B*) containing bath solutions. Data are normalized to the maximum tail current in Na^+ and aspartate ($n = 4$). The *inset* gives a representative recording used for this analysis with Na^+ and aspartate.

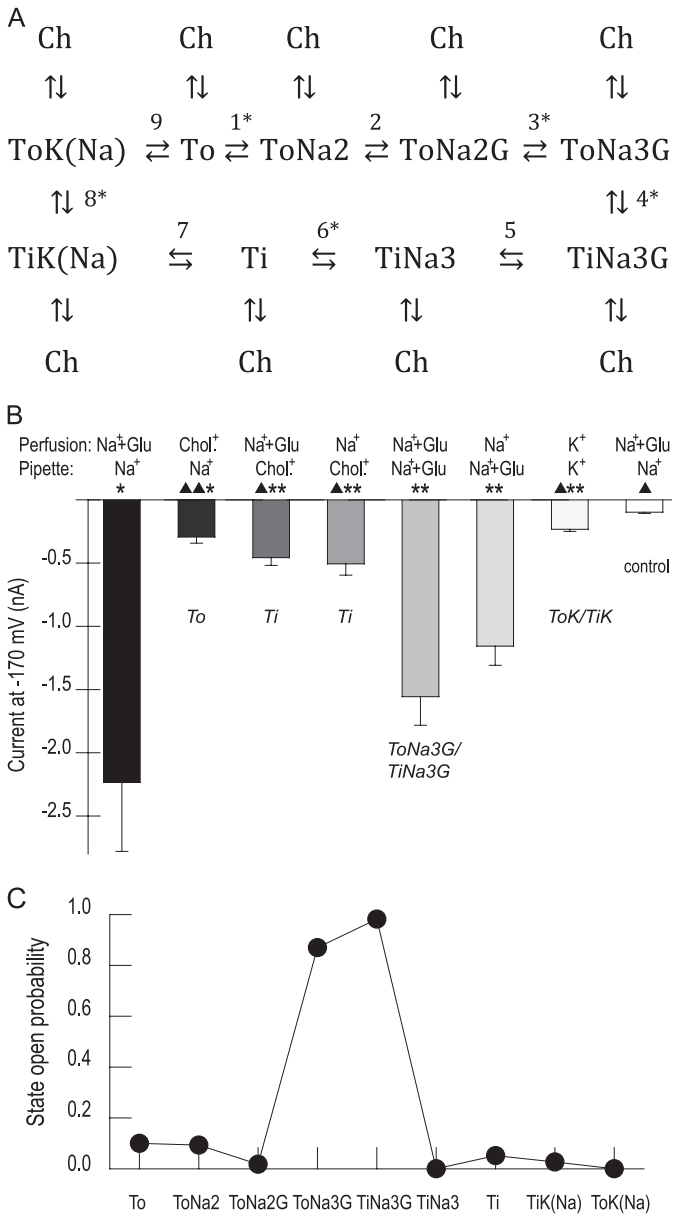

FIGURE 5. **A kinetic model of substrate-dependent channel gating.** *A*, state diagram of the transport cycle (*ToX*, outward-facing transporter; *TiX*, inward-facing transporter; *Ch*, open channel states). Transition within the uptake cycle are *numbered 1–9* (electrogenic reactions marked with an *asterisk*). *B*, steady-state absolute current amplitudes of cells expressing EAAT4 at −170 mV for various internal and external substrate conditions. Cells were dialyzed and perfused with the given pipette or bath solution to force the transporter into specific states of the transport cycle (in *italic*). For solutions without alkali cations, choline nitrate was used as substituent. When glutamate was applied from both sides of the membrane, a concentration of 30 mM was used, otherwise 1 mM was used. Based on a Student's *t* test, *asterisks* and *triangles* indicate statistically significant differences from control measurements with untransfected cells or from measurements with cytoplasmic Na^+ and extracellular Na^+/glutamate, respectively (*one symbol*, $p < 0.05$; *two symbols*, $p < 0.01$) ($n = 4–8$). *C*, state-specific open probabilities of each transporter state determined by global fitting of the model shown in *A*.

open probabilities were smaller than with glutamate. Moreover, a leftward shift of the voltage dependence was also observed. With Li^+ alone, tail currents were similar to those with external Na^+.

Kinetic Model of Substrate-dependent Channel Gating—We next tested whether all new data on substrate-dependent gating of EAAT4 anion currents obtained in our study could be satisfactorily described with a kinetic model in which all substrate-dependent gating processes are conferred by transitions within the uptake cycle. If this were the case, relative open probabilities, time courses of current relaxations, and concentration-response curves with glutamate, aspartate, and cysteine in the presence of Na^+ as well as of Li^+, could be fitted by a kinetic scheme that is based on the EAAT transport cycle with certain states resulting in opening of the anion channel.

Our kinetic scheme (Fig. 5*A*) is based on the well understood transport mechanism of mammalian isoforms, in agreement with other models describing EAAT glutamate transporters (5, 25, 26). Glutamate transporters can exist in two structurally distinct conformations, outward- and inward-facing (26). Each substrate can bind to the outward-facing as well as to the inward-facing conformation. Glutamate uptake is initiated by association of three Na^+, one H^+, and one glutamate. Consecutively, a large portion of the transporter, the "translocation domain," performs a substantial inward movement, resulting in the inward-facing conformation (26). After release of the substrates, internal

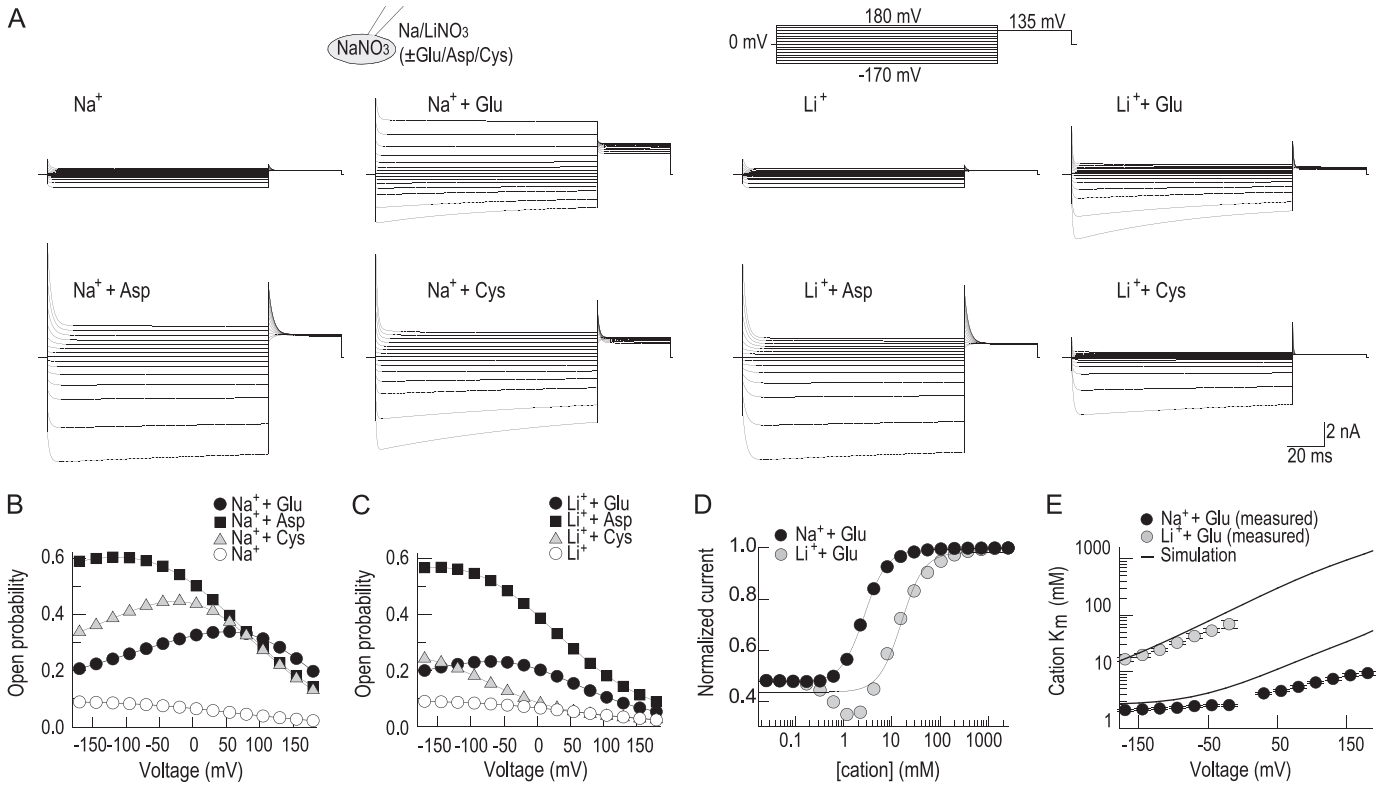

FIGURE 6. **Reproduction and prediction of experimental EAAT4 data.** *A*, simulated current traces upon voltage steps for various conditions. *B* and *C*, simulated activation curves. *D*, simulated concentration-response curves of Na^+ and Li^+ in the presence of 20 mM glutamate at −170 mV. Fits of Hill equations yielded K_D values of 2.7 mM (Na^+) and 15.8 mM (Li^+) and Hill coefficients of 1.8 (Na^+) and 1.9 (Li^+). *E*, predicted voltage dependence of simulated apparent cation K_D values (*lines*) in comparison with experimental values (*circles*).

cation binding permits retranslocation from the inward-facing to the outward-facing conformation.

Because we used buffered solutions at only one pH in our experiments, we simplified the scheme by omitting H^+ binding and lumping together several binding steps to a single reaction. Moreover, because transporter retranslocation is also possible with internal Na^+ (14), we allowed internal Na^+ to substitute for K^+ in state *TiK(Na)* required for transporter retranslocation. This change does not violate the dependence of net transport on internal K^+, as rate-limiting retranslocation rates with Na^+ were 30- to 100-fold smaller than those in the presence of internal K^+ and thus negligible. The binding order of cations in the outward-facing as well as in the inward-facing conformation was taken from a recent study by Zhang and co-workers (27). As in earlier reports, cation binding reactions and transporter translocation were allowed to be electrogenic (5).

Different apparent substrate affinities justified the use of separate parameter sets for substrate-binding reactions for each amino acid. Because radioactive uptake experiments with EAAT4 exhibited lower transport rates for L-aspartate than for L-glutamate (8), substrate translocation (R4) might also differ between substrates. As cations appeared to interact with substrates in our measurements (Figs. 3 and 4), we assumed distinct cation-binding rates (R3) to the substrate-liganded transporter for each amino acid substrate (23). Finally, as association of the third cation appears to be the basis of cation specificity (28), the model assumes distinct rate constants for reaction R3 with Na^+ or Li^+. All parameters (rate constants R1–R7, R9) were then optimized against experimentally obtained relative open probabilities, time courses of current relaxations, and concentration dependences of glutamate, aspartate, and cysteine with Na^+ or Li^+.

To account for voltage- and substrate-dependent EAAT4 anion currents, we introduced channel modes Ch in which EAAT anion channels are open. No transitions between different channel modes were permitted so that the uptake cycle cannot proceed as long as the channel is open (22). Overall, channel open probabilities were given as sums of fractional occupancies in channel model Ch, and time and voltage dependences of EAAT4 currents were then calculated using published unitary EAAT4 current amplitudes (22). To compare measured relative open probabilities with simulated absolute values, we found that an open probability ~0.6 was the highest value the model could assume to correctly reproduce time-dependent channel gating (Fig. 6). For the model optimization, we therefore normalized relative P_o to this value.

We allowed all transport states to reach the channel mode and simply determined the intrinsic open probability of each state by model optimization. However, our initial data set did not allow unambiguous determination of opening reactions of each single state and yielded several parameter sets with vastly different open probabilities of single states that fitted experimental data similarly well (data not shown). We therefore conducted additional experiments to further constrain the possible parameter space for the model optimization. Using various combinations of pipette and bath solutions to specifically force

TABLE 1

Parameters of the EAAT4 model

Rate constants of the transport process and channel gating at 0 mV. Electrogenic reactions are defined by zδ values, which correspond to the product of the charge, and the fraction of the electric field the charge is moved across the membrane. Clockwise transitions in the model scheme are denoted as "forward reactions." Where amino acid-specific rates are used, values are given in parenthesis in order (glutamate; aspartate; cysteine).

no.	Forward reaction	Backward reaction	zδ
1	237 · 10^3 M^{-2} s^{-1}	275 · 10^0 s^{-1}	0.33
2	(75.0; 176; 18.6) · 10^6 M^{-1} s^{-1}	(10.1; 1.67; 12.5) · 10^3 s^{-1}	
3(Na)	(16.3; 1.79; 4.85)· 10^3 M^{-1} s^{-1}	(0.80; 0.98; 2.46) · 10^3 s^{-1}	0.33
3(Li)	(3.30; 1.08; 1.17)· 10^3 M^{-1} s^{-1}	(6.30; 1.17; 13.6) · 10^3 s^{-1}	0.33
4	(1.66; 0.20; 0.91)· 10^1 s^{-1}	(14.6; 15.5; 70.0) · 10^2 s^{-1}	0.51
5	(249; 250; 8.25) · 10^4 s^{-1}	n. d.	
6	34.5 · 10^0 s^{-1}	1.38 · 10^6 M^{-3} s^{-1}	0.56
7	24.8 · 10^6 M^{-1} s^{-1}	3.32 · 10^3 s^{-1}	
8	1.4 · 10^0 s^{-1}	1.0 · 10^{-2} s^{-1}	0.27
9	14.4 · 10^3 s^{-1}	842 · 10^3 M^{-1} s^{-1}	

State open probability

To:	0.10	TiNa3:	0.00
ToNa2:	0.09	Ti:	0.05
ToNa2G:	0.02	TiK:	0.03
ToNa3G:	0.87	ToK:	0.00
TiNa3G:	0.98		

the transporter into several states of the transport cycle, we were able to evaluate state-specific open probabilities. The kinetic scheme predicts that transporters with cytoplasmic Na^+ lacking external cations accumulate in state To, whereas transporters exposed to cation-free internal solutions in presence of external Na^+ reside in Ti (Fig. 5*B*). Both conditions led to current amplitudes that were small, but significantly larger than background currents from untransfected cells (Fig. 5*B*). Cells perfused with Na^+ and high concentrations (30 mM) of glutamate are expected to predominantly assume ToNa3G/TiNa3G. As expected, this led to 5–10-fold larger current amplitudes (Fig. 5*B*) as under conditions without glutamate. Finally, measurements with K^+ on both sides of the membrane also resulted in low current amplitudes. We therefore constrained channel open probabilities at states TiK, ToK, Ti, and To to be below 10% for the optimization of the model, whereas open probabilities of the other states could be freely adjusted by the optimization procedure.

Global fitting yielded a set of parameters that reproduced the time, voltage, and substrate dependences of EAAT4 anion currents (Figs. 5*C* and 6 and Table 1). Fitted anion channel opening probabilities were highest for the glutamate-bound states ToNa3G/TiNa3G. We were unable to distinguish anion channel gating between these two states because we did not find any experimental condition that resulted in exclusive accumulation in ToNa3G or in TiNa3G. All other states, including the K^+-bound states TiK and ToK, exhibit very small open probabilities. This result is in contrast to other EAAT models that attributed significant channel functions to the state TiK (14), but experimentally well supported by the very small EAAT4 anion current amplitudes in symmetric K^+ (Fig. 5*B*). Our experiments and the kinetic model show that all amino acid substrate-free states of the transporter contribute to a small tonic conductance and that the current increase after glutamate application is due to channel opening from the glutamate-bound states.

As an additional test, we used the resulting kinetic model to predict voltage dependences of apparent dissociation constants for Na^+ and Li^+ (Fig. 6*E*). The model correctly predicts the apparently increased electrogenicity of Li^+ binding as compared with Na^+ (Fig. 1*E*). Simulated K_D values resemble experimental values quantitatively with a slight deviation at positive potentials and in their voltage dependence (Fig. 6*E*). These results demonstrate that changes in distribution among different transporter states with Li^+ modify the apparent voltage dependence of cation binding.

DISCUSSION

EAAT glutamate transporters are dual function proteins that mediate secondary-active glutamate transport and pore-mediated anion conduction (7, 8, 10, 13, 22, 29). We sought to study the relationship between the glutamate transport cycle and anion channel gating by selectively modifying the transport process at specific steps. We analyzed EAAT4 anion currents under subsequent perfusion of cells with various amino acid substrates and cations and tested whether changes in anion channel gating could be explained in terms of variable interactions of the different substrates with the transporter.

Li^+ and Na^+ are both alkali metals, and Li^+ is capable of substituting for Na^+ in a variety of biological processes. For EAAT, studies have revealed isoform-specific cation specificity. EAAT2 function is sodium-specific (28), and the strict Na^+ specificity of EAAT2 was attributed to serine 440 in EAAT2, which corresponds to a glycine in the other members of the EAAT family. Mutating this amino acid located at the tip of hairpin 2 (25, 30) to glycine or performing the reverse mutation in the EAAT3 background permitted or prohibited Li^+ to drive transport (28). In EAAT1 and EAAT3, Li^+ was reported to support coupled transport but apparently not anion currents (20, 21). We decided to reanalyze the effects of Li^+ because these earlier results indicated cation-dependent anion channel gating beyond the uptake cycle. We found that Li^+ was fully capable of supporting EAAT4 anion currents (Figs. 1 and 3). Anion currents were active in the absence of glutamate with similar amplitudes in external Li^+ and Na^+. Application of glutamate increased anion currents in Na^+ as well as in Li^+. Cells expressing EAAT4 exhibited even larger instantaneous anion currents when perfused with Li^+ and aspartate than with Na^+ and glutamate.

We also performed such experiments with EAAT1. Our results demonstrated that, with Li^+, glutamate is only capable of activating EAAT1 anion channels at negative, but not at positive voltages (Fig. 2). These findings explain why EAAT1 anion currents in Li^+ were not detected in *Xenopus* oocytes. To separate coupled and uncoupled EAAT currents in oocytes, inward currents are usually attributed to coupled uptake and outward currents to anion currents. The exclusive Li^+-induced increase of EAAT1 anion currents at negative potentials was thus difficult to be detected. Our findings suggest that Li^+ supports anion channel activity in all EAAT isoforms except EAAT2, albeit with distinct voltage dependence of anion channel activity.

We found that glutamate, aspartate, and cysteine activated EAAT4 anion currents with different voltage and time dependences (Figs. 1, 3, and 4). This finding might suggest that channel opening and closing reactions are directly gated by substrate binding. Various experimental results argue against this interpretation. First, differences in channel activation persisted at saturating amino acid concentrations indicating that variations in substrate association are not sufficient to explain distinct gating. Second, sequences of apparent binding affinities were not identical to orders of current amplitudes, *i.e.* with cysteine as the least affine substrate in Na^+, is still nearly as effective as aspartate in inducing anion currents (Fig. 3*C*). Third, although aspartate and cysteine differed in net charge at neutral pH, gating with aspartate and cysteine was relatively similar in Na^+. Fourth, no reasonable fit of the model to our data (Fig. 5*A*) was possible if the transporter was solely allowed to assume distinct binding/unbinding rates for each amino acid (data not shown).

We next tested whether our experimental data could be reproduced by a kinetic scheme that is based on the uptake cycle. We used global parameter optimization with uncoupled currents as the sole experimental input using measurements under multiple experimental conditions. This approach generated parameters that reproduced the time, voltage, and substrate dependence of EAAT4 anion currents and predicted the observed electrogenicity of apparent Na^+ and Li^+ binding (Fig. 6). The kinetic parameters show that Li^+ binds with slower association and faster dissociation rates than Na^+ (Table 1). Comparable results were obtained for binding of glutamate, aspartate, and cysteine. Moreover, these data indicate that interactions between cations and amino acid substrates could be modeled by modifying cation binding rates depending on the nature of the bound substrate. Consistent with reports about different transport rates for glutamate and aspartate (8), the fitted model assumes different translocation rates (R4) for each amino acid.

The model differs in certain aspects from a kinetic scheme recently developed for EAAT4 from an analysis of the relaxation of transport-associated currents upon rapid application of glutamate (18). In this study, EAAT4 was considered to be unique in its voltage dependence of transporter retranslocation. According to Mim *et al.* (18), this reaction step was promoted by hyperpolarization in EAAT1–3, whereas in EAAT4, positive potentials increased the rate of retranslocation. However, our model could fit the presented data only with an effective inward movement of positive charge accompanying retranslocation that is accelerated at negative potential, as believed for other EAAT isoforms. Whereas Mim *et al.* (18) varied relative conductances between different anion-conducting states, we assigned identical unitary anion conductances. This assumption is based on the recent finding that unitary EAAT4 anion currents determined by noise analysis are identical in the presence as well as in the absence of glutamate (22). In a kinetic scheme developed for EAAT2 (14), translocation from the outward to the inward-facing conformation was assumed to be electroneutral, in contrast to our finding. Electrogenic translocation is in agreement with recent structural information (25, 26) that predicts a substantial transmembrane movement of a large portion of the transporter, the so-called "translocation domain" (26). Such translocations through an electric field are expected to be electrogenic (31).

As amino acid binding appeared to be voltage-independent (24, 32), electrogenicity of the transport process (two elementary charges) should be distributed among Na^+ binding and translocation steps. Assuming electrogenic Na^+ binding and unbinding as well as transporter translocation and retranslocation, our kinetic scheme satisfactorily mimics the voltage dependence of measured anion currents (Fig. 6 and Table 1) and the experimentally observed changes of activation curves upon changing amino acid substrates. It correctly predicts differences in the apparent voltage dependence of cation binding (Fig. 6*E*). These findings support the notion that a major fraction of substrate-specific voltage dependence observed in EAAT anion channels arises from electrogenic cation association. Due to interactions between substrates and cations, various amino acids apparently change the voltage dependence of anion channel opening by modulating these electrogenic reactions.

The substrate efficacy was different in Li^+ than in Na^+. In Li^+, aspartate remained a strong agonist, glutamate became quite weaker, whereas cysteine was changed to a very poor agonist (Fig. 3). The voltage dependence of anion channel activation was also changed by Li^+, resulting in a shift of the activation curves (Fig. 4) to more negative values. We conclude that open probabilities of EAAT4 anion channels depend on interactions between cations and substrates. Consistently, mathematical modeling (Figs. 5 and 6 and Table 1) demonstrated that changes in substrate-induced gating could be explained by differences in substrate-binding, association of the third cation to the substrate-bound transporter and translocation rates that are all subject to the respective amino acid species. All of these parameters had to be modified to acquire satisfying fits of the model (Fig. 6). A recent study, in which apparent affinities of glutamate, aspartate and cysteine in sodium and lithium were determined for EAAT3 uptake and shown to be individually dependent on the nature of the cation (23), has demonstrated a similar interaction of cations and amino acid substrates.

Taken together, our results remove remaining doubts about the absence of anion channel gating processes beyond the transport cycle and demonstrate that, for a large variety of substrate conditions, EAAT4 gating can be adequately described assuming an intimate coupling to the transport cycle. EAAT4 anion channels obtain their substrate and voltage dependence exclusively from transitions within the glutamate uptake cycle. There are additional anion-dependent gating transitions (22) besides substrate-dependent processes. EAAT anion channels can be well described by a kinetic model in which only amino acid substrate-bound states exhibit high anion channel open probabilities. These data clarify similarities and differences of glutamate transporter-associated anion channels and ligand-gated anion channels. EAAT anion channels predominantly tend to open from amino acid-bound states. The distribution between these and other states depends on cation and substrate con-

centrations and on the membrane potential, resulting in a complex regulation of EAAT anion current amplitudes.

Acknowledgments—We thank Drs. S. Amara and J. Rothstein for providing the expression constructs for human EAAT1 and rat EAAT4. We appreciate helpful discussions with Drs. David Ewers, Alexi Alekov, Ariane Leinenweber, Jasmin Hotzy, Gabriel Stölting, Nicole Schneider, and Natalie Winter.

REFERENCES

1. Torres, G. E., and Amara, S. G. (2007) *Curr. Opin. Neurobiol.* **17,** 304–312
2. Kanner, B. I. (2006) *J. Membr. Biol.* **213,** 89–100
3. Grewer, C., Gameiro, A., Zhang, Z., Tao, Z., Braams, S., and Rauen, T. (2008) *IUBMB. Life* **60,** 609–619
4. Levy, L. M., Warr, O., and Attwell, D. (1998) *J. Neurosci.* **18,** 9620–9628
5. Zerangue, N., and Kavanaugh, M. P. (1996) *Nature* **383,** 634–637
6. Fairman, W. A., and Amara, S. G. (1999) *Am. J. Physiol.* **277,** F481–F486
7. Wadiche, J. I., Amara, S. G., and Kavanaugh, M. P. (1995) *Neuron* **15,** 721–728
8. Fairman, W. A., Vandenberg, R. J., Arriza, J. L., Kavanaugh, M. P., and Amara, S. G. (1995) *Nature* **375,** 599–603
9. Watzke, N., and Grewer, C. (2001) *FEBS Lett.* **503,** 121–125
10. Melzer, N., Biela, A., and Fahlke, Ch. (2003) *J. Biol. Chem.* **278,** 50112–50119
11. Amara, S. G., and Fontana, A. C. (2002) *Neurochem. Int.* **41,** 313–318
12. Melzer, N., Torres-Salazar, D., and Fahlke, Ch. (2005) *Proc. Natl. Acad. Sci. U.S.A.* **102,** 19214–19218
13. Wadiche, J. I., and Kavanaugh, M. P. (1998) *J. Neurosci.* **18,** 7650–7661
14. Bergles, D. E., Tzingounis, A. V., and Jahr, C. E. (2002) *J. Neurosci.* **22,** 10153–10162
15. Ryan, R. M., Mitrovic, A. D., and Vandenberg, R. J. (2004) *J. Biol. Chem.* **279,** 20742–20751
16. Huang, S., and Vandenberg, R. J. (2007) *Biochemistry* **46,** 9685–9692
17. Otis, T. S., and Kavanaugh, M. P. (2000) *J. Neurosci.* **20,** 2749–2757
18. Mim, C., Balani, P., Rauen, T., and Grewer, C. (2005) *J. Gen. Physiol.* **126,** 571–589
19. Tao, Z., Zhang, Z., and Grewer, C. (2006) *J. Biol. Chem.* **281,** 10263–10272
20. Huang, S., Ryan, R. M., and Vandenberg, R. J. (2009) *J. Biol. Chem.* **284,** 4510–4515
21. Borre, L., and Kanner, B. I. (2001) *J. Biol. Chem.* **276,** 40396–40401
22. Kovermann, P., Machtens, J. P., Ewers, D., and Fahlke, Ch. (2010) *J. Biol. Chem.* **285,** 23676–23686
23. Menaker, D., Bendahan, A., and Kanner, B. I. (2006) *J. Neurochem.* **99,** 20–28
24. Torres-Salazar, D., and Fahlke, Ch. (2006) *J. Neurosci.* **26,** 7513–7522
25. Yernool, D., Boudker, O., Jin, Y., and Gouaux, E. (2004) *Nature* **431,** 811–818
26. Reyes, N., Ginter, C., and Boudker, O. (2009) *Nature* **462,** 880–885
27. Zhang, Z., Tao, Z., Gameiro, A., Barcelona, S., Braams, S., Rauen, T., and Grewer, C. (2007) *Proc. Natl. Acad. Sci. U.S.A.* **104,** 18025–18030
28. Zhang, Y., and Kanner, B. I. (1999) *Proc. Natl. Acad. Sci. U.S.A.* **96,** 1710–1715
29. Larsson, H. P., Picaud, S. A., Werblin, F. S., and Lecar, H. (1996) *Biophys. J.* **70,** 733–742
30. Boudker, O., Ryan, R. M., Yernool, D., Shimamoto, K., and Gouaux, E. (2007) *Nature* **445,** 387–393
31. Parsegian, A. (1969) *Nature* **221,** 844–846
32. Grewer, C., Watzke, N., Wiessner, M., and Rauen, T. (2000) *Proc. Natl. Acad. Sci. U.S.A.* **97,** 9706–9711